A Diagnostic Calculator for Detecting Glaucoma on the Basis of Retinal Nerve Fiber Layer, Optic Disc, and Retinal Ganglion Cell Analysis by Optical Coherence Tomography

José Manuel Larrosa,[1] Javier Moreno-Montañés,[2] José María Martinez-de-la-Casa,[3] Vicente Polo,[1] Álvaro Velázquez-Villoria,[2] Clara Berrozpe,[3] and Marta García-Granero[4]

[1]Ophthalmology Service, Hospital Universitario Miguel Servet, Faculty of Medicine, University of Saragossa, Saragossa, Spain
[2]Department of Ophthalmology, Clínica Universidad de Navarra, Faculty of Medicine, Universidad of Navarra, Pamplona, Spain
[3]Ophthalmology Service, Hospital Clínico San Carlos, Faculty of Medicine, Universidad Complutense de Madrid, Madrid, Spain
[4]Unidad de Estadística, Department of Biochemistry and Genetics, University of Navarra, Pamplona, Spain

Correspondence: Javier Moreno-Montañés, Department of Ophthalmology, Clínica Universidad de Navarra, Av. Pío XII, 36, Pamplona, Spain;
jmoreno@unav.es.

JML, JM-M, and JMM-d-l-C contributed equally to the work presented here and should therefore be regarded as equivalent authors.

Purpose. The purpose of this study was to develop and validate a multivariate predictive model to detect glaucoma by using a combination of retinal nerve fiber layer (RNFL), retinal ganglion cell-inner plexiform (GCIPL), and optic disc parameters measured using spectral-domain optical coherence tomography (OCT).

Methods. Five hundred eyes from 500 participants and 187 eyes of another 187 participants were included in the study and validation groups, respectively. Patients with glaucoma were classified in five groups based on visual field damage. Sensitivity and specificity of all glaucoma OCT parameters were analyzed. Receiver operating characteristic curves (ROC) and areas under the ROC (AUC) were compared. Three predictive multivariate models (quantitative, qualitative, and combined) that used a combination of the best OCT parameters were constructed. A diagnostic calculator was created using the combined multivariate model.

Results. The best AUC parameters were: inferior RNFL, average RNFL, vertical cup/disc ratio, minimal GCIPL, and inferior-temporal GCIPL. Comparisons among the parameters did not show that the GCIPL parameters were better than those of the RNFL in early and advanced glaucoma. The highest AUC was in the combined predictive model (0.937; 95% confidence interval, 0.911–0.957) and was significantly ($P = 0.0001$) higher than the other isolated parameters considered in early and advanced glaucoma. The validation group displayed similar results to those of the study group.

Conclusions. Best GCIPL, RNFL, and optic disc parameters showed a similar ability to detect glaucoma. The combined predictive formula improved the glaucoma detection compared to the best isolated parameters evaluated. The diagnostic calculator obtained good classification from participants in both the study and validation groups.

Keywords: glaucoma diagnosis, OCT, optic disc, retinal ganglion cell, retinal nerve fiber layer

Glaucoma is a frequent cause of blindness worldwide.[1] The modern standard for diagnosing glaucoma is based on analyses of structural and functional changes of the optic nerve head (ONH). Visual field analysis is the functional study used most widely. Structural changes in the optic nerve are observed using different techniques. Optic disc photography conventionally has been used to evaluate the structural optic nerve damage in glaucoma; however, interobserver variability and moderate interobserver agreement suggest that fundus photography discriminates poorly between normal and glaucomatous optic nerves.[2] Advances in ocular imaging techniques, principally the advent of optical coherence tomography (OCT), have facilitated assessment of the peripapillary retinal nerve fiber layer (RNFL). Different OCT methods have been introduced for quantitative and qualitative analyses of the RNFL, using glaucoma algorithms to measure the thickness along a 3.4-mm-diameter circle centered on the optic disc. Recently, advances in OCT segmentation algorithms have facilitated the measurement of the thickness of the macular retinal ganglion cells-inner plexiform layers (GCIPL).[3–5] Essentially, glaucoma causes retinal ganglion cell bodies and their axons to die. Current published studies have suggested that analysis of the macular GCIPL yields the same glaucoma diagnostic result as RNFL thickness.[3–5]

Recent articles have analyzed combinations of different structural parameters to improve the diagnostic ability to detect glaucoma; some analyzed the RNFL thickness and optic nerve parameters and others the peripapillary RNFL and macular GCIPL parameters.[6–8] The purpose of the current study was to develop and validate multivariate predictive models to detect glaucoma by using a combination of optic nerve evaluation, RNFL thickness, and macular GCIPL parameters measured by Cirrus OCT (Carl Zeiss Meditec, Inc., Dublin, CA, USA) to improve the detection of glaucoma in the initial and advanced disease stages.

MATERIALS AND METHODS

Patients with normal or glaucomatous eyes were recruited prospectively in three departments of ophthalmology: the Clínica Universidad de Navarra, Pamplona, Spain; Hospital Clínico S. Carlos, Universidad Complutense, Madrid, Spain; and Hospital Miguel Servet, Universidad of Saragossa, Saragossa, Spain. Institutional review boards/ethics committees approved the study. According to the committee, no written informed consent was needed for the glaucoma group because data were collected from regular clinical practice. All normal volunteers provided informed consent before entering the study, which adhered to the Declaration of Helsinki.

Complete ophthalmic examinations of all participants were performed, which included slit-lamp biomicroscopy, IOP measurement, dilated stereoscopic fundus examination, gonioscopy, and standard automated perimetry using the 24-2 Swedish interactive threshold algorithm (Humphrey field analyzer, Carl Zeiss Meditec, Inc.). All participants were Caucasian-Hispanic and had a spherical equivalent within 5.0 diopters (D) or less, astigmatism of 3.00 D or less, best-corrected visual acuity (VA) of 20/40 or better; no corneal or retinal pathology, amblyopia, or macular disease; no contraindication to pupillary dilation or intolerance to topical anesthetic or mydriatic agents; and no substantial media opacity.

The glaucoma group included patients with a clinical diagnosis of open-angle glaucoma identified by gonioscopy and visual field defects and an IOP that exceeded 21 mm Hg on at least 3 different days. The visual field was classified as glaucomatous according to a glaucoma staging system (GSS), a modified version of the Hodapp-Parrish-Anderson classification.[9] This classification allows for stage assignment based on visual field damage. Stage 0 indicates ocular hypertension, stage 1 early glaucoma, stage 2 moderate glaucoma, stage 3 advanced glaucoma, stage 4 severe glaucoma, and stage 5 blindness. Visual field damage was reproducible in at least three reliable and consecutive visual field tests performed on different days. In patients with bilateral glaucoma, only a randomized eye was included. The normal group included participants with an IOP of 21 mm Hg or lower, normal visual fields, and no familial history of glaucoma. The normal group included participants without ocular diseases consecutively recruited from hospital staff members, nurses, relatives of patients, and patients referred for a routine VA examination.

OCT Acquisition and Analysis

After pupillary dilation with 1% tropicamide, an OCT evaluation using Cirrus OCT was performed on the same day as visual field analysis. Before the study, the manufacturer calibrated the OCTs at the three hospitals. The experienced operators who performed the OCT examinations differed from the examiner who performed visual field testing and was masked to the other findings.

Three OCT volume scans (200 × 200 axial scans) centered on the optic disc were obtained for each eye. Retinal nerve fiber layer data were evaluated automatically using the Cirrus OCT system software version 6.0. After optic discs were scanned, three new scans (200 × 200 axial scans) were obtained in the macular cube to analyze GCIPLs. The OCT signal strength also was analyzed. Only the best signal strength scan from the three obtained scans was selected for the RNFL and GCIPLs analysis.

The optic nerve cube evaluated the RNFL thickness and optic disc parameters. Retinal nerve fiber layer parameters evaluated were the global RNFL average (micrometers) and RNFL thickness in the superior, inferior, nasal, and temporal quadrants. The 12-hour clock positions were not included. The optic disc parameters were the rim area (mm²), average cup/disc (C/D) ratio, vertical C/D ratio, and cup volume (mm³).

The macular cube in Cirrus OCT combined the thicknesses of the GCIPL layers and the inner plexiform layer, because the Cirrus software cannot distinguish between the two, and the combined thickness indicates the health of the GCIPLs. The GCIPL data analyzed from the macular cube were the average, minimal (lowest GCIPL thickness over a single meridian crossing the annulus), and sectoral (superotemporal, superior, superonasal, inferonasal, inferior, inferotemporal) thicknesses measured in an elliptical annulus around the fovea. The vertical dimension was 0.5 to 2 mm from the fovea, and the horizontal dimension was 0.6 to 2.4 mm from the fovea.

Cirrus software automatically organized all RNFL, optic disc parameters, and GCIPL values into three groups: within normal limits (green), borderline (yellow), and out of normal limits (red). Only cases with a signal strength of 6 or higher were analyzed. Cases with signal strength of 5 or lower were rejected.

Data Study Analysis

Five hundred eyes (248 right, 252 left eyes) of 500 participants (251 men, 249 women) were enrolled. The mean ± standard deviation (SD) age was 68.3 ± 8.7 years. One hundred fifty-one eyes were normal, 124 eyes had ocular hypertension (grade 0 according to the GSS classification), and 215 eyes were glaucomatous. The mean ± SD age in the normal group was 67.7 ± 7.7 years and 69.2 ± 9.9 years in the glaucomatous group ($P = 0.065$).

Data Validation Analysis

One hundred eighty-seven eyes (93 right, 94 left eyes) of 187 participants (91 men, 96 women) were included in this group. This validation group was created at the same time as the study group so that 500 eyes were chosen for the analysis group and the other eyes for the validation group. Eyes were distributed randomly in both groups. Fifty-seven eyes were normal, 48 eyes were hypertensive, and 82 were glaucomatous. The mean ± SD age in the normal group was 67.0 ± 9.2 years and 69.7 ± 11.4 years in the glaucomatous group ($P = 0.072$). Demographic data from the study and validation groups are shown in Table 1. No statistical differences were found between the groups in any evaluated parameters.

Statistical Analysis

The Shapiro-Wilk test was used to assess the normality of the quantitative variables. Normally distributed variables were summarized using means ± SD, and nonnormally distributed variables were summarized using median and interquartile ranges (25th and 75th percentiles). To compare quantitative variables between two independent groups (sex, normal/glaucomatous group), the Mann-Whitney U test was used for nonnormally distributed variables (all but age), and the two-sample Student's t-test was used for normally distributed variables (age only). The χ^2 test was used to compare qualitative variables between independent groups.

Three different predictive models were evaluated using multivariate logistic regression: one from the quantitative data from the RNFL, optic disc, and GCIPLs (model 1); another using qualitative data (green, yellow, and red [model 2]), and combined qualitative and quantitative data (model 3). These models were analyzed in the study and validation groups. The receiver operating characteristic curves (ROC) were used to determine the discriminatory capabilities between healthy and

TABLE 1. Demographic Data From the Study and Validation Groups

Data	Study Group	Validation Group	P Value
No. of cases	500	187	
Mean ± SD age, y	68.3 ± 8.7	68.2 ± 10.4	0.83
Mean ± SD visual field index	80.0 ± 32.1	85.1 ± 21.6	0.12
No. of women (%)	249 (49.8)	96 (51.3)	0.93
No. of right eyes (%)	248 (49.6)	93 (49.7)	0.97
No. of glaucomatous eyes (%)	215 (43)	82 (43.9)	0.95
GSS (%)			
Stage 1	92 (42.7)	37 (45.1)	0.53
Stage 2	71 (33)	21 (25.6)	
Stage 3	36 (16.7)	16 (19.5)	
Stage 4	16 (7.4)	7 (8.5)	
Stage 5	0	1 (1.2)	

GSS, glaucoma staging system.

glaucomatous eyes. The best parameters from the RNFL, optic disc, and GCIPL analyses were compared to the multivariate models in early moderate and advanced glaucoma. AUCs were compared using the Hanley-McNeil method for paired data.[10] Sensitivities of 85% and 95% fixed specificities were calculated.

Bootstrapping also was used to internally validate the regression model and was implemented by constructing a number of resamples ($k = 100$) of the dataset (of equal size) obtained by random sampling with replacement from the original dataset.[11] Bootstrapping allows use of a complete dataset for model development, evaluation, and validation and currently is considered the resampling method of choice.[12] Data were evaluated using SPSS version 20.0.1 software (SPSS, Inc., Chicago, IL, USA), STATA version 12.0 software (Stata Corp, College Station, TX, USA), and MedCalc version 11.2 (MedCalc Software, Mariakerke, Belgium).

RESULTS

Areas Under the ROC Curves

Table 2 shows AUC values, best sensitivity and specificity values, and sensitivity for the 85% and 95% fixed specificities from the RNFL and optic disc values from the study group. The best AUCs were the RNFL inferior quadrant (AUC, 0.867; 95% confidence interval [CI], 0.835–0.896), and the average RNFL (AUC, 0.849; 95% CI, 0.815–0.880); however, the RNFL inferior quadrant sensitivity is higher for

the 85% and 95% fixed specificities than the average RNFL. The best AUC of the optic disc was the vertical C/D ratio (AUC, 0.820; 95% CI, 0.783–0.863) with values similar to the rim area.

Areas under the curve of the GCIPL values in the study group are shown in Table 3. The best AUCs were the minimal value GCIPL (AUC, 0.868; 95% CI, 0.835–0.896), the inferior temporal quadrant GCIPL (AUC, 0.867; 95% CI, 0.834–0.896), and the average GCIPL (AUC, 0.837; 95% CI, 0.801–0.868). Comparison of the RNFL inferior quadrant and average RNFL with the minimal value GCIPL and inferior quadrant GCIPL did not show significant differences, suggesting that GCIPL analysis does not improve the ability to diagnose glaucoma based on the RNFL thickness.

In the study group, glaucoma was classified according to the GSS system. Early moderate glaucoma was defined as grades 1 and 2 and advanced glaucoma as grades 3, 4, and 5. Comparisons between the AUCs of the best RNFL thickness and those of the best GCIPL thicknesses did not identify significant differences in early moderate and advanced glaucoma (Table 4).

New Multivariate Predictive Models

The best predictive parameters of the RNFL, optic disc, and GCIPLs were selected based on multivariate regression analysis, and three models were obtained. Model 1 included quantitative data, model 2 qualitative data, and model 3

TABLE 2. Area Under the ROCs, Best Sensitivity–Specificity Balance, Sensitivity for 85% and 95% Fixed Specificities of the RNFL and Optic Disc Values in the Study Group (RNFL and Optic Disc Parameters)

Site	AUC (95% CI)	P Value	Sensitivity%/Specificity%	Sensitivity by Specificity, %	
				85% Specificity	95% Specificity
RNFL					
Average	0.849 (0.815–0.880)	0.0001	80.4/78.9	71.0	50.5
Superior	0.814 (0.778–0.848)	0.0001	69.3/83.7	65.6	49.4
Inferior	0.867 (0.835–0.896)	0.0001	80.5/80.7	74.4	56.3
Temporal	0.681 (0.639–0.722)	0.0001	52.6/82.5	48.8	25.6
Nasal	0.646 (0.602–0.688)	0.0001	62.8/62.8	33.0	14.4
Optic disc					
Rim area	0.819 (0.791–0.861)	0.0001	67.4/85.9	67.9	54.0
Average C/D ratio	0.787 (0.749–0.822)	0.0001	64.6/85.9	63.7	40.0
Vertical C/D ratio	0.820 (0.783–0.863)	0.0001	64.2/89.1	67.4	54.9
Cup volume	0.708 (0.666–0.748)	0.0001	72.5/63.8	41.9	17.7

TABLE 3. Area Under the ROCs, Best Sensitivity–Specificity Balance, Sensitivity for 85% and 95% Fixed Specificities of GCIPL Values in the Study Group (Ganglion Cell Thickness)

Site	AUC (95% CI)	*P* Value	Sensitivity%/Specificity%	Sensitivity by Specificity, %	
				85% Specificity	95% Specificity
Average	0.837 (0.801–0.868)	0.0001	81.8/74.3	66.1	40.9
Superior	0.795 (0.757–0.829)	0.0001	69.7/76.4	57.6	34.4
Inferior	0.836 (0.802–0.869)	0.0001	67.9/89.1	71.1	48.3
Superotemporal	0.814 (0.777–0.847)	0.0001	66.5/84.8	64.5	33.0
Superonasal	0.747 (0.706–0.784)	0.0001	72.1/67.6	46.1	29.8
Inferotemporal	0.867 (0.834–0.896)	0.0001	74.5/85.9	73.2	59.1
Inferonasal	0.796 (0.758–0.831)	0.0001	74.4/72.2	56.3	42.8
Minimum	0.868 (0.835–0.896)	0.0001	88.4/72.2	73.4	44.7

combined qualitative and quantitative data. Table 5 and Figure 1A show the AUCs of the three models. Model 3 obtained the best AUC. We exported data to Stata 12 and compared models using Fitstat software. The output shows that the combined model 3 was considered the simplest, according to the Bayesian information criterion (BIC). Because of space limitations, only the model 3 formula is shown here:

Model 3 predicted probability =

$$e^{\wedge}(0.905 + 0.044 \times age - 1.477 \times (SNGCC = yellow)$$
$$- 1.190 \times (SNGCC = red) + 1.403 \times (STGCC = yellow)$$
$$+ 1.095 \times (STGCC = red) + 1.455 \times (MCGC = yellow)$$
$$+ 1.109 \times (MCGC = red) + 0.006 \times (CDAC = yellow)$$
$$+ 2.231 \times (CDAC = red) + 0.583 \times (CDAC = gray)$$
$$- 0.034 \times ITGC - 0.035 \times IRNFL - 0.099 \times CDA \, (\times 100)$$
$$+ 0.117 \times VCD \, (\times 100)) / (1 + e^{\wedge}(0.905 + 0.044 \times age$$
$$- 1.477 \times (SNGCC = yellow) - 1.190 \times (SNGCC = red)$$
$$+ 1.403 \times (STGCC = yellow) + 1.095 \times (STGCC = red)$$
$$+ 1.455 \times (MCGC = yellow) + 1.109 \times (MCGC = red)$$
$$+ 0.006 \times (CDAC = yellow) + 2.231 \times (CDAC = red)$$
$$+ 0.583 \times (CDAC = gray) - 0.034 \times ITGC - 0.035$$
$$\times IRNFL - 0.099 \, CDA \, (\times 100) + 0.117 \times VCD \, (\times 100)))$$

where SNGCC is the superonasal GCIPL color; STGCC is the superotemporal GCIPL color; MCGC is the minimal GCIPL color; CDAC C/D ratio is average color; ITGC is the inferotemporal GCIPL value; IRNFL is the inferior quadrant RNFL value; CDA C/D is the average value; and VCD is the vertical C/D value.

We suggest the following cutoff points: predicted probability of <0.3 is the low probability; 0.3 to 0.6 is the intermediate probability range; and >0.6 is high probability. In the study group, only 9.3% of eyes with a low score were glaucomatous, 41% of eyes with an intermediate score were glaucomatous, and finally, 91% of the high-score group were glaucomatous. In the validation group, the percentages were 9.3%, 52%, and 91%, respectively. Therefore, the proposed cutoffs points seem adequate.

Table 6 shows the odds ratios (ORs) of the best parameters of the GCIPLs, optic disc, and RNFL obtained in the combined multivariate linear regression model. The ROC from model 3 and best parameters of the RNFL, optic disc, and GCIPL analysis in the study group are shown in Figure 1. AUCs of model 3 were significantly (P < 0.001) higher than all the best parameters evaluated (Table 7), suggesting that the ability to detect glaucoma using the multivariate model is better than the best parameters of the RNFL, optic disc, and GCIPL analysis.

Figure 2 shows the ROC curve in patients with early moderate and advanced glaucoma. In early glaucoma, model 3 obtained significantly higher AUCs than all isolated parameters evaluated (P < 0.001). However, in advanced glaucoma, model 3 AUCs were only higher than three parameters: the minimal

TABLE 4. Area Under the ROCs, Best Sensitivity-Specificity Balance, Sensitivity for 85% and 95% Fixed Specificities of RNFL and GCIPL Values in Early and Advanced Glaucomas (Study Group)

Site	AUC (95% CI)	*P* Value	Sensitivity%/Specificity%	Sensitivity by Specificity, %	
				85% Specificity	95% Specificity
Early-moderate glaucoma					
Average RNFL	0.871 (0.828–0.907)	0.0001	77.3/87.1	77.9	53.5
Inferior RNFL	0.877 (0.834–0.921)	0.0001	77.3/86.4	77.7	59.8
Vertical C/D ratio	0.843 (0.796–0.882)	0.0001	73.6/84.8	72.3	53.6
Minimal GCIPL	0.868 (0.824–0.905)	0.0001	86.5/77.3	73.6	39.7
Infero-temporal GCIPL	0.869 (0.825–0.905)	0.0001	69.4/92.4	76.1	60.1
Advanced glaucoma					
Average RNFL	0.936 (0.891–0.967)	0.0001	86.3/91.7	91.7	76.5
Inferior RNFL	0.933 (0.887–0.964)	0.0001	88.5/92.4	93.2	84.2
Vertical C/D ratio	0.911 (0.860–0.948)	0.0001	84.6/90.9	88.6	78.9
Minimal GCIPL	0.928 (0.881–0.961)	0.0001	86.5/93.2	88.4	63.9
Infero-temporal GCIPL	0.953 (0.911–0.978)	0.0001	86.6/94.2	92.3	86.5

TABLE 5. Area Under the ROCs, Best Sensitivity-Specificity Balance, Sensitivity for 85% and 95% Fixed Specificities of New Predictive Multivariate Model

Model	AUC (95% CI)	P Value	Sensitivity%/Specificity%	Sensitivity by Specificity, %	
				85% Specificity	95% Specificity
Study group					
Model 1	0.912 (0.883–0.935)	0.0001	85.1/84.5	84.2	68.4
Model 2	0.926 (0.898–0.948)	0.0001	91.3/83.7	89.3	67.4
Model 3*	0.937 (0.911–0.957)	0.0001	83.8/91.2	87.9	77.8
Validation group					
Model 1	0.926 (0.879–0.959)	0.0001	81.7/95.2	86.6	81.7
Model 2	0.937 (0.892–0.967)	0.0001	82.9/96.1	86.6	82.9
Model 3	0.932 (0.886–0.963)	0.0001	84.1/93.3	87.8	78.1

* Differences between models 1 and 3 in AUC = 0.0268 (95 CI, 0.0100–0.0436; $P = 0.0017$).

GCIPL ($P = 0.01$), inferior temporal GCIPL ($P = 0.04$), and average RNFL ($P = 0.04$).

Validation Analysis

The three regression models were analyzed in the validation group and the calculated AUCs were similar to those obtained for the study group; in all models, the AUCs were higher than 0.90 (Table 5). To facilitate the external validation of model 3, we include the Website from which to download the Excel (Microsoft, Redmond, WA, USA) formula with the diagnostic categories (http://www.oftared.com/docs/Glaucoma%20Diagnostic%20Calculator.xlsx, in the public domain) (Fig. 3).

FIGURE 1. (**A**) The ROC from the three predictive models. (**B**) The ROC from the best parameters of the RNFL, optic disc, and GCIPLs and the new parameter (model 3) in all eyes.

The bootstrap method was the internal validation method, and its estimates agreed closely with the parameters obtained by regression analysis of the original dataset. Furthermore, the bootstrap estimate of the AUC from model 1 was 0.918 (95% CI, 0.891–0.943), 0.934 (95% CI, 0.909–0.957) from model 2, and 0.922 (95% CI, 0.917–0.938) from model 3.

DISCUSSION

Advances in OCT technology have enabled more detailed and precise quantitative assessment of glaucomatous structural changes, through circumpapillary RNFL thickness measurements and, more recently, GCIPL thickness measurements. Considering the current results, GCIPL assessment does not improve the ability to diagnose glaucoma from the peripapillary RNFL evaluation. These results generally agreed with previous reports.[13–15] However, RNFL and GCIPL assessments target different neuroretinal areas, and they may be potentially complementary to overcome the incidence of false positive results of some OCT RNFL parameters.[16] Thus, in Cirrus OCT, Leal-Fonseca et al.[16] reported an 11% false positive rate in the average RNFL color code and 13% in the superior and inferior quadrants and average C/D ratio. This supports the combined use of parameters from different retinal areas for diagnosing glaucoma. Consequently, multivariate models predictive of glaucoma have been proposed to improve the diagnostic ability of these OCT parameters that yield results that are highly correlated and somewhat redundant. Previous studies have used learning classifiers, linear discriminant functions, principal component analysis, and logistic regression analyses[6–8] to improve the OCT diagnostic value. Some studies combined ONH and RNFL parameters that evaluated the status of GC axons at different locations,[17] whereas other studies combined ONH, RNFL, and macular GCIPL complex parameters, which accumulate information about different retinal anatomic areas.[6–8] However, those studies did not show the mathematical functions in their reports or provide a Web link to allow external validation or simple implementation of the proposed function in a given patient. It is important that such information be accessible; otherwise, the value of the function is limited to the authors and cannot be compared.

We performed an internal validation of the formula, which ensured that the proposed model was robust and guaranteed that the function would be useful in future datasets. In addition, compared to previous reports,[6–8,17] we presented our diagnostic calculator for external validation directly and through a Web link. We also tested and validated the functions in larger populations compared with comparable reports such as that of Mwanza et al.[8] (687 subjects compared to 253
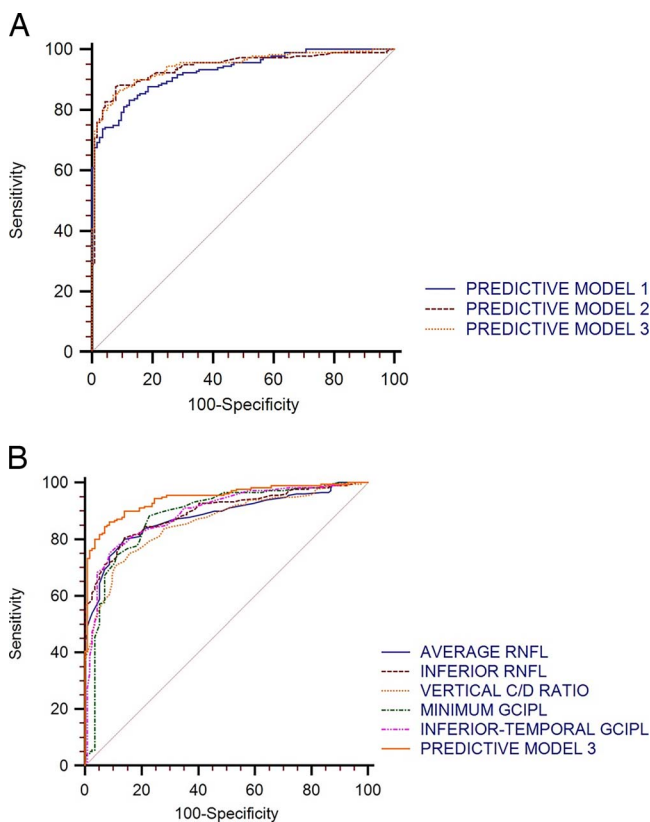
TABLE 6. Odds Ratio (95% CI) of the Best Parameters of the GCIPL, Optic Disc Parameters, and RNFL Values Obtained by Combined Multivariate Logistic Regression (Model 3)

| Characteristic	Beta	SE (B)	Wald Test	P Value	OR	95% CI Lower	95% CI Upper
Age, y	0.044	0.015	8.647	**0.003**	1.045	1.015	1.076
Superonasal GCIPL color (vs. green)			6.483	**0.039**			
Yellow	−1.477	0.611	5.842	**0.016**	0.228	0.069	0.756
Red	−1.190	0.745	2.547	0.111	0.304	0.071	1.312
Superotemporal GCIPL color (vs. green)			7.114	**0.029**			
Yellow	1.403	0.568	6.102	**0.014**	4.067	1.336	12.378
Red	1.095	0.642	2.910	0.088	2.990	0.850	10.523
Minimal GCIPL color (vs. green)			8.216	**0.016**			
Yellow	1.455	0.554	6.906	**0.009**	4.285	1.448	12.686
Red	1.109	0.556	3.985	**0.046**	3.033	1.020	9.012
Cup/disc ratio average color (vs. green)			16.593	**0.001**			
Yellow	0.006	0.494	1.3E-04	0.991	1.006	0.382	2.649
Red	2.231	0.565	15.563	**<0.001**	9.305	3.072	28.184
Gray	0.583	0.523	1.242	0.265	1.791	0.643	4.992
Inferotemporal GCIPL value	−0.034	0.017	3.913	**0.048**	0.967	0.935	1.000
Inferior RNFL thickness	−0.035	0.008	19.459	**<0.001**	0.966	0.951	0.981
Average C/D ratio, value × 100	−9.864	3.274	9.076	**0.003**	0.906	0.869	0.944
Vertical C/D ratio, value × 100	11.718	3.312	12.519	**<0.001**	1.124	1.078	1.172
Constant	0.905	1.861	0.237	0.627			

P values in bold are significant. OR, odds ratio; SE (B), standard error of beta.

subjects). Furthermore, our subjects were recruited from three hospitals and were representative of the Spanish population. Finally, the availability of our function allows it to be compared in larger populations and with different ethnic and sociogeographic features.

The function significantly improved the diagnostic value of the single OCT parameters (Table 7). It is interesting that the RNFL parameters, such as the average RNFL or inferior RNFL, had AUCs (0.849 and 0.867, respectively) similar to the best GCIPL parameters, such as the minimal and inferior-temporal GCIPLs (AUCs, 0.868 and 0.867, respectively), whereas the ONH parameters such as the vertical C/D ratio had smaller AUC areas. However, the factor with the highest OR in the multivariate model was the C/D ratio average color (Table 6). The C/D ratio adds information to the model about an anatomical feature that does not overlap with other measurements of RNFL or GCIPL parameters. In contrast, the RNFL and GCIPL parameters assess different aspects of the RNFL thickness that are correlated strongly between them. The multivariate model includes the most relevant factors; in the current study, the GCIPL parameters had more weight in the formula (better odds ratios [ORs]) than the RNFL parameters

TABLE 7. Differences in the AUC Among the Best Quantitative Parameters From the RNFL or From the GCIPL and Combined Predictive Parameter (Model 3) in the Study Group

Model Comparison	Differences Between AUCs	95% CI	P Value
Model 3 vs. average RNFL	0.0818	0.0551–0.108	<0.0001
Model 3 vs. inferior quadrant RNFL	0.0641	0.0384–0.0899	<0.0001
Model 3 vs. minimal GCIPL	0.0688	0.0416–0.0961	<0.0001
Model 3 vs. inferotemporal GCIPL	0.0517	0.0233–0.0802	<0.0001
Model 3 vs. vertical C/D ratio	0.103	0.0684–0.137	<0.0001
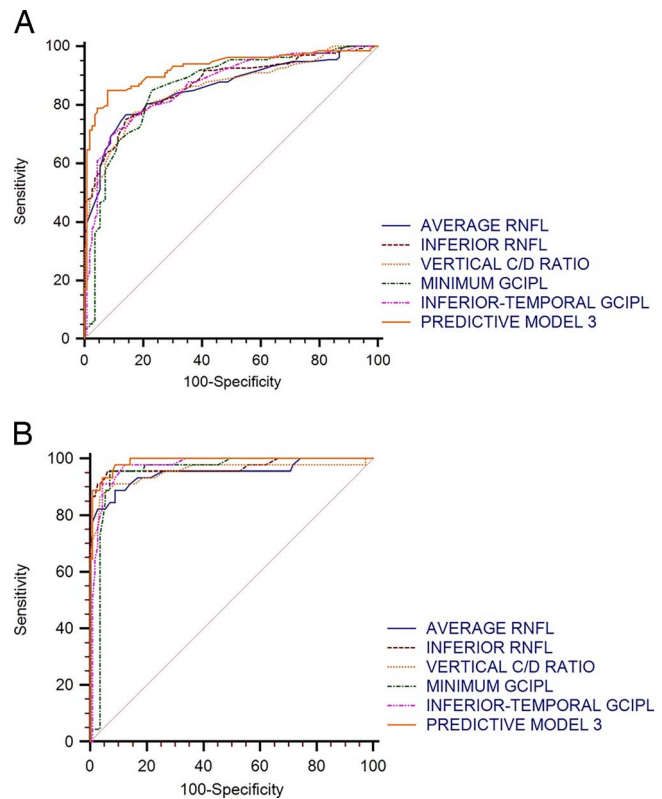
FIGURE 2. (A) The ROC from the best parameters of the RNFL and GCIPLs and a new parameter (model 3) in early moderate glaucoma. (B) The ROC from the best parameters of the RNFL and GCIPLs and a new parameter (model 3) in advanced glaucoma.
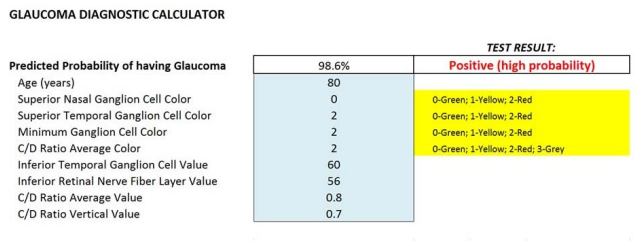
FIGURE 3. Printout of an Excel file from one case combining the nine parameters of the glaucoma diagnostic calculator (*blue*). The automatic positive result indicates a high probability of glaucoma.

(Table 6). Therefore, GCIPL assessment showed that the peripapillary RNFL thickness evaluation was more advantageous for diagnosing glaucoma. The low RNFL ORs in the formula suggested that the information about these parameters do not add much to the GCIPL measurements and supported the idea that the RNFL and GCIPL data mainly overlap.

Performing OCT often depends on the disease severity. It is easier to distinguish advanced glaucoma stages, but the function should not be restricted to detection in patients with early or moderate glaucoma. This approach avoids restricting the range in the test measures and therefore attenuating correlations among variables that can result in falsely low estimates of factor loading. The current function was not limited to early damage but covers all disease stages, unlike other reports.[8] Compared to reports that included patients with all degrees of glaucoma severity,[17] we also provided the diagnostic performance in the early-moderate and advanced stages. The diagnostic ability of the proposed multivariate function outperforms the diagnostic value of single parameters in early moderate and advanced glaucoma (Figs. 1, 2).

Models 2 and 3 showed similar levels of performance in the study series, and it is true that quantitative outcomes are usually preferred to categorizations, suggesting that perhaps the simpler model should be preferred. However, in this case, we must bear in mind that the qualitative measurements are not simply cutoff values of the original quantitative ones but are attributes provided by the Cirrus OCT (as indicated by the manufacturer), which take into account more patient information (like age and optic disc size) to assign a result to a given category. Thus, the information provided by the quantitative measurement is enriched (like the "gray" category, which indicates that the optic disc size is unusually small or big). Therefore, model 3 was finally selected for the Excel calculator.

The current study had limitations. All subjects were from the same geographic region despite the large number of participants and involvement of three hospitals from different cities. However, the availability of our formula through a Web link allows future testing of the function in different geographic and ethnic settings, similar to other OCT normative databases before being included in any software. The diagnostic color codes are based on the commercial version of the Cirrus OCT currently available. Their normative databases may be updated and modified in the future, and the results should not be extrapolated directly to other OCT devices. Another limitation of the proposed function was that subjects with macular disease, such as age-related macular degeneration (AMD), were excluded. Age-related macular degeneration is a relevant condition that may be considered in glaucoma suspects. The important weight of the GCIPL parameters in the formula should be considered and, therefore, implementation of this function in the presence of any macular condition is not strongly recommended. Despite these limitations, this diagnostic calculator is easy to use (Fig. 3) and includes only 9 parameters and the optic disc size as a gray color code, indicating a size not evaluated by Cirrus OCT. The
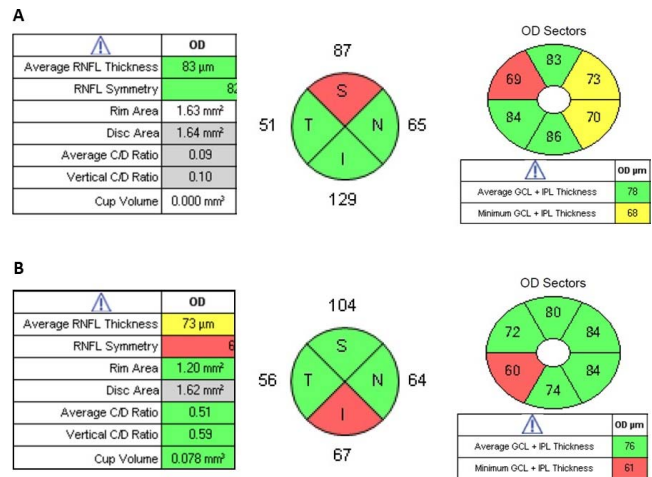
FIGURE 4. Optical coherence tomography images of two cases of suspected early glaucoma (right eyes) with normal visual fields. (**A**) *Left*: Average RNFL and optic disc parameters with values within normal limits. *Middle*: RNFL quadrants with superior quadrant out of normal limits (*red*). *Right*: GCIPL areas with temporal superior area out of normal limits (*red*) and borderline nasal areas (*yellow*). The minimum GCIPL is borderline. In this case, the glaucoma diagnostic calculator value was 2.7%, indicating a low predictive probability of glaucoma. (**B**) *Bottom left*: Borderline average RNFL (*yellow*) and within normal limits of optic disc parameters (*green*). The disc area was 1.62 mm², which is similar to that in case A. *Middle*: RNFL quadrants with inferior quadrant out of normal limits (*red*). *Right*: GCIPL areas with temporal inferior area out of normal limits (*red*). The minimum GCIPL is *red*. In this case, the glaucoma diagnostic calculator value was 75.2%, suggesting a high probability of glaucoma.

formula may also assist the diagnosis of early glaucoma in cases with artifacts in the qualitative OCT analysis (Fig. 4), and it provides a new parameter that can facilitate, in addition to other tests, the glaucoma diagnosis in the clinical practice.

In conclusion, the GCIPL and RNFL parameters had similar diagnostic value, while the combined function increased the diagnostic value of these single parameters. The combined model includes information from 8 parameters from three structures, ONH, peripapillary RNFL, and GCIPLs, and requires only 1 minute to determine the probability of glaucoma in a suspected patient using the diagnostic calculator. The function is applicable even in large and small optic discs that do not show color classification in the OCT report (gray). In light of these results, the use of predictive models using a combination of parameters from Cirrus OCT improves glaucoma detection. The availability of the multivariate function allows external validation in other datasets (from different racial and geographic origins) and its potential use in clinical practice as another tool to interpret the OCT data analysis.

References

1. Quigley HA. Number of people with glaucoma worldwide. *Br J Ophthalmol*. 1996;80:389–393.

2. Azuara-Blanco A, Katz LJ, Spaeth GL, et al. Clinical agreement among glaucoma experts in the detection of glaucomatous changes of the optic disk using simultaneous stereoscopic photographs. *Am J Ophthalmol*. 2003;136:949–950.

3. Tan O, Chopra V, Lu AT, et al. Detection of macular ganglion cell loss in glaucoma by Fourier-domain optical coherence tomography. *Ophthalmology*. 2009;116:2305–2314.

4. Kim NR, Lee ES, Seong GJ, et al. Structure-function relationship and diagnostic value of macular ganglion cell complex measurement using Fourier-domain OCT in glaucoma. *Invest Ophthalmol Vis Sci*. 2010;51:4646–4651.

5. Mwanza JC, Durbin MK, Budenz DL, et al. Glaucoma diagnostic accuracy of ganglion cell-inner plexiform layer thickness: comparison with nerve fiber layer and optic nerve head. *Ophthalmology*. 2012;119:1151–1158.

6. Huang JY, Pekmezci M, Mesiwala N, Kao A, Lin S. Diagnostic power of optic disc morphology, peripapillary retinal nerve fiber layer thickness, and macular inner retinal layer thickness in glaucoma diagnosis with Fourier-domain optical coherence tomography. *J Glaucoma*. 2011;20:87–94.

7. Fang Y, Pan YZ, Li M, Qiao RH, Cai Y. Diagnostic capability of Fourier-domain optical coherence tomography in early primary open angle glaucoma. *Chin Med J (Engl)*. 2010;123:2045–2050.

8. Mwanza JC, Warren JL, Budenz DL, et al. Combining spectral domain optical coherence tomography structural parameters for the diagnosis of glaucoma with early visual field loss. *Invest Ophthalmol Vis Sci*. 2013;54:8393–8400.

9. Mills RP, Budenz DL, Lee PP, et al. Categorizing the stage of glaucoma from pre-diagnosis to end-stage disease. *Am J Ophthalmol*. 2006;141:24–30.

10. Hanley JA, McNeil BJ. A method of comparing the areas under receiver operating characteristic curves derived from the same cases. *Radiology*. 1983;148:839–843.

11. Efron B, Tibshirani RJ. *An Introduction to the Bootstrap*. London, UK: Chapman & Hall; 1993.

12. Brunelli A, Rocco G. Internal validation of risk models in lung resection surgery: bootstrap versus training-and-test sampling. *J Thorac Cardiovasc Surg*. 2006;131:1243–1247.

13. Medeiros FA, Zangwill LM, Bowd C, Vessani RM, Susanna R Jr, Weinreb RN. Evaluation of retinal nerve fiber layer, optic nerve head, and macular thickness measurements for glaucoma detection using optical coherence tomography. *Am J Ophthalmol*. 2005;139:44–55.

14. Leung CK, Chan WM, Yung WH, et al. Comparison of macular and peripapillary measurements for the detection of glaucoma: an optical coherence tomography study. *Ophthalmology*. 2005;112:391–400.

15. Wollstein G, Schuman JS, Price LL, et al. Optical coherence tomography (OCT) macular and peripapillary retinal nerve fiber layer measurements and automated visual fields. *Am J Ophthalmol*. 2004;138:218–225.

16. Leal-Fonseca M, Rebolleda G, Oblanca N, Moreno-Montañes J, Muñoz-Negrete J. A comparison of false positives in retinal nerve fiber layer, optic nerve head and macular ganglion cell-inner plexiform layer from two spectral-domain optical coherence tomography devices. *Graefes Arch Clin Exp Ophthalmol*. 2014;252:321–330.

17. Baskaran M, Ong EL, Li JL, et al. Classification algorithms enhance the discrimination of glaucoma from normal eyes using high-definition optical coherence tomography. *Invest Ophthalmol Vis Sci*. 2012;53:2314–2320.

Investigative Ophthalmology & Visual Science